UDC 621.39
doi:10.15217/issn1684-8853.2017.1.72

OPTIMIZATION OF ERROR CONCEALMENT BASED ON ANALYSIS OF FADING TYPES
Part 1: Statistical Description of the Wireless Video Channel, Models of BER Determination and Error Concealment of Video Signals

***Ofer Hadar*[a],** *PhD, Associate Professor, hadar@cse.bgu.ac.il*
***Irina Bronfman*[a],** *MSc Student, irinamo@post.bgu.ac.il*
***Nathan Blaunstein*[a,b],** *Dr. Sc., Phys.-Math., Professor, nathan.blaunstein@hotmail.com*
[a]*Ben-Gurion University of the Negev, POB 653, 1, Ben Gurion St., Beer Sheva, 74105, Israel*
[b]*Jerusalem College of Technology — Lev Academic Center, 21 Havaad Haleumi, P.O.B. 16031, Jerusalem, 91160, Israel*

Purpose: *This work is based on the recent research investigations in the combination of two subjects: Fading and Error Concealment. The main aim of the work is to present a more effective method of calculations of fading channel's parameters and to devise methods of achieving of better and more effective performance of Error Concealment, which will lead to higher quality of the video signals after passing through the fading channel.* ***Methods:*** *We explore the influence of fading on a communication channel, by studying the Gaussian, Gaussian, and Ricean distributions. Additionally, we explore existing methods of prediction and of Error Concealment and their influence on the video quality after its exit from the fading channel.* ***Results:*** *It is demonstrated that the Ricean distribution is broader and that it includes the other distributions, Gaussian (ideal channel) and Rayleigh (channel with a strong fading). Therefore, this distribution is used for tests of practical cases occurring in the video channel. On the issue of Error Concealment, a method of Symmetrical CALIC which is an optimization of the CALIC method, was implemented and compared with the original CALIC and with other methods. It has been determined that the proposed optimization yields better results than all the methods used for comparison. In addition, a new method of Error Concealment, named Balanced Percentage Calculation, is proposed. In comparison, its results are two times better on average than the results of Symmetrical CALIC, and are much better than the results of other methods used. Two themes have been combined in such a way that fading influenced the appearance of errors in the video. Those errors have been replaced by the proposed methods of Error Concealment. All practical tests and comparisons were performed using the MatLab.* ***Practical relevance:*** *The proposed method of calculations of fading channel's parameters allows to perform calculations for all types of channels. This method significantly facilitates work with channels in general and with necessary calculations for channels in particular. The suggested optimization of the existing method of Error Concealment and the new proposed method of Error Concealment allow to receive higher quality video after passing through the fading channel.*

Keywords *— Ricean Distribution, Ricean Fading, Bit Error Rate, Error Concealment, Level Crossing Rate, Average Fade Duration, CALIC, Symmetrical CALIC, Balanced Percentage Calculation, Weighted Averaging, Intra Prediction using System of Linear Equations.*

Introduction

This article is based on the research of a combination of two fields: Fading and Error Concealment (EC).

Initially, the impact of three types of fading — Gaussian, Rayleigh and Ricean — in the communication channel is investigated. Typically, studies use the Rayleigh distribution for the description of the worst situation in the channel and the Gaussian distribution for the description of the best (ideal) situation in the channel. In this work, we propose using the modification of the Ricean distribution for the description of all situations in the channel. The work demonstrates that the Ricean distribution is much broader than the Gaussian and the Rayleigh types, and incorporates the latter distributions. Therefore, in the practical section of this paper, the tests and the effects of fast fading are performed using the Ricean distribution.

In addition, Symmetrical CALIC, which constitutes an optimization of one of the existing methods of EC named CALIC (Context-based, Adaptive, Lossless Image Codec) [1], has been introduced. A comparative analysis versus the original CALIC and versus the other methods is performed, and its outcome determines that the proposed optimization gives better results than all the methods used for comparison. Additionally, a new method of EC, called Balanced Percentage Calculation is proposed. The comparative analysis shows that in terms of average signal estimations, this method performs twice as well as the Symmetrical CALIC, and much better than other methods used for comparison.

There are many works on processing and transmitting video over wireless communication channels. For example, [2] proposes an adaptive hybrid digital-analog video transmission scheme for robust video streaming in mobile networks with realistic fading channels. This scheme differs from other researches by not assuming wireless channels to be Gaussian, which is critical for fading channels [3] proposes a joint source-channel coding scheme for the delivery of scalable video over Multi Input Multi Output (MIMO) wireless systems. In it, aiming to improve the power efficiency of the MIMO-system, authors explore how to allocate sub-channels and transmit power to the video layers under constraints of video quality and delay. [4] analyzes the impact of bit errors on the perceived video quality. This impact depends on error resilience of the data format, EC mechanism used and characteristics of the bit error pattern. In tests the authors implement various error resilient tools at the transmitter side and at the receiver. Errors that require interactive feedback on dynamic channel conditions are discussed. [5] presents a rate-optimization procedure for the transmission of scalable video sequences of the H.264/AVC standard over wireless channels. Currently existing studies present neither a wireless channel with Ricean fading nor the influence of this type of fading on the appearance of errors in the video file, whereas our study addresses this issue.

There is also a lot of research on the topic of EC for video and especially on EC for video transmitted over wireless channels. For instance, [6] presents an EC system for overcoming visible distortions in video sequences which are transmitted over a losses prone communication network. This system provides an EC solution from the point of receiving the transmitted sequence by the decoder without human interference. [7] presents a hybrid EC algorithm for compressed video sequences, based on temporal and spatial concealment methods. The article develops post-processing techniques for the reconstruction of missing or damaged macroblocks. The authors propose a support of decision tree for efficiently choosing the best appropriate EC method, according to the spatial and temporal characteristics of the sequence. [8] studies the effectiveness of Flexible Macroblock Ordering in mitigating the impact of errors on the decoded video and proposes solutions to improve the EC on H.264 decoders. Study [9] proposes hybrid EC technique. In spatial domain, three methods: Weighted Average Interpolation, Directional Interpolation and Transformed Based Concealment are implemented and compared on various noises. To reduce the computational complexity and better quality, proposed a hybrid spatial-temporal video EC technique is proposed. It includes mode selection based on boundary matching decision. [10] presents a progressive block matching algorithm (PBMA) that performs EC in order to recover visual quality. The PBMA utilizes the Euclidean distance to consider the affection of corrupted-residual in block matching principle. The PBMA successively recovers the corrupted macroblock with minimizing the impact of corrupted-residual by Euclidean distance information. Prior to our work, EC by symmetrical method has not been introduced in a previous study. Moreover, the CALIC method [1], on which the Symmetrical CALIC Concealment method is based, has not been used for EC, only for the prediction of the lost pixels. We also considered the possibility of using this method for both asymmetric and symmetric EC. In addition, no one has previously used balanced calculations to perform EC, a method proposed and tested in our work.

The main aim of the work is devising a method for more accurate analysis of EC. This goal was achieved as can be seen in the results of practical simulation.

The first Section's work deals with the background and defines the main goal of the work. The second section of this article presents a theoretical base of Slow and Fast fading, and Temporal and Spatial EC Methods. The third section presents Mathematical and Statistical Description of Wireless Channel with fading. The fourth section constitutes a description of Modified and New Models of EC in Channel with Fading. The fifth section of the article talks about the simulation, the sixth section shows the comparative results of the calculations, and the seventh section summarizes the work and gives recommendations for future research.

The article is divided into two parts. First (this) part presents statistical description of the wireless video channel, existing and modified models of Bit Error Rate (BER) determination and existing models of EC of video signals. Second part presents a description of modified and new models of EC of video signals in channel with fading, and then it shows the practical simulation and its results.

Overview

Slow and Fast Fading

Slow fading. The slow variations of spatial signals (expressed in decibels, dB) typically have a lognormal distribution or Gaussian distribution (expressed in watts, W) [11–19]. The probability density function (PDF) of the signal changes in accordance with the corresponding standard deviation and with the mean over a certain period of time or in a separate small area. This function depends on the nature of the terrain and on the nature of the atmospheric and ionospheric conditions. This PDF is determined by:

$$PDF(r)=\frac{1}{\sigma_L\sqrt{2\pi}}\exp\left\{-\frac{(r-\bar{r})^2}{2\sigma_L}\right\}, \tag{1}$$

where r is the value of the received signal strength or voltage envelope; $\bar{r}=\langle r\rangle$ is the mean value of the random signal level; $\sigma_L=\left\langle r^2-\left(\bar{r}\right)^2\right\rangle$ is the variance or time-average power ($\langle r\rangle$ indicates the averaging operation of a variable r of the received signal envelope).

Fast fading. In the case of a stationary transmitter and receiver (static multipath channel), due to multiple reflections and scattering from various obstacles surrounding the transmitter and receiver, the radio signals travel along different paths of varying lengths, thereby producing such fast deviations from the signal strength (in volts, V) or power (in watts) at the receiver.

In the case of dynamic multipath situation, subscribers' antenna is moving, and the spatial variation of the resultant signal at the receiver can be regarded as the time variations [20, 21]. The signal received by the mobile antenna at any point in space may consist of a plurality of signals having randomly distributed amplitudes, phases and angles of signal arrival, as well as different time delays. All these features change the relative phase shift depending on the spatial position and, finally, lead to signal fading in the space domain. In the dynamic (mobile) multipath situation, the signal fading happens in the mobile receiver in the time domain. This is a temporary fading due to the frequency shift of the emitted stationary transmitter. In fact, the changes in time or dynamic changes of the propagation path lengths associated with the Doppler effect, which is created due to relative movement between the stationary base station and the moving subscriber.

To illustrate the effects of changes in the phase in the time domain due to the Doppler frequency shift (Doppler effect [11–19]), let consider a helicopter moving at a constant velocity V along the path XY (Fig. 1). The difference in path lengths driven by the signal from the source S to a mobile phone at the points X and Y is $\Delta l = l\cos\theta = V\Delta t\cos\theta$, where Δt is the time required for moving receiver to move from point X to point Y along the way, and θ is the angle between the mobile direction along the XY and the direction to the source at the current point Y, that is, YS. The change of phase of the resultant received signal is created due to the difference in path length, thus:

$$\Delta\Phi = k\Delta l = \frac{2\pi}{\lambda} l\cos\theta = \frac{2\pi V\Delta t}{\lambda}\cos\theta. \quad (2)$$

Hence it is evident that a change of the radiated frequency, or Doppler shift, is given by f_D:

$$f_D = \frac{1}{2\pi}\frac{\Delta\Phi}{\Delta t} = \frac{V}{\lambda}\cos\theta. \quad (3)$$

It is important to note from Fig. 1, that the angles at points X and Y are equal only when the corresponding lines XS and YS are parallel. Therefore, this figure is valid only in the limit, when the terminal S is far away from the moving antenna at the points X and Y. The maximum Doppler shift is $f_{D_{\max}} = V/\lambda$, it is denoted as f_m here.

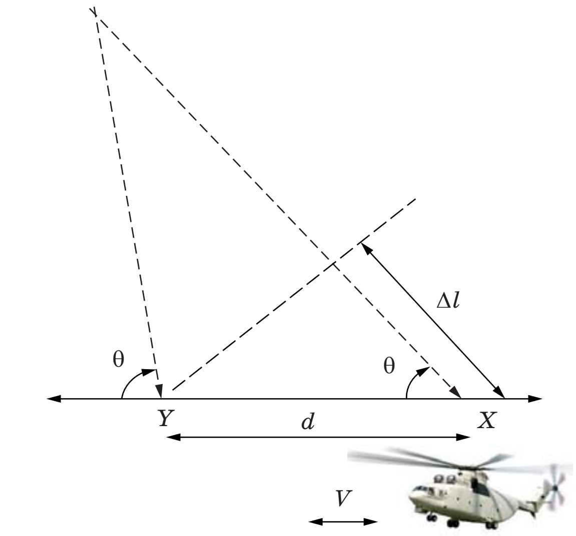

■ ***Fig. 1.*** Geometry of the mobile link for Doppler effect estimation

There exist a large number of probability distribution functions that could be used to describe the fast fading effects, such as Rayleigh, Suzuki, Ricean, Gamma, Gamma-Gamma and etc. The Ricean distribution is very general [11–19] as it includes both the line-of-sight (LOS) with scattering and diffraction and the non-LOS. In order to evaluate the contribution of each component of the signal at the receiver, i.e. dominant (or LOS) and secondary (or multipath), the Ricean parameter K is usually introduced as a ratio between these components [11–19], i.e.:

$$K = \frac{LOS - Component\ power}{Multipath - Component\ power}. \quad (4)$$

The Ricean PDF distribution of the signal strength or voltage envelope r can be defined as [1–19]:

$$PDF(r) = \frac{r}{\sigma^2}\exp\left\{-\frac{r^2 + A^2}{2\sigma^2}\right\} I_0\left(\frac{Ar}{\sigma^2}\right)$$
$$\text{for } A > 0,\ r \ge 0, \quad (5)$$

where σ is the standard deviation of signal envelope; A is the peak strength or voltage of the dominant component envelope; $I_0(\cdot)$ is the modified Bessel function of the first kind and zero-order.

According to (4), it's possible rewrite the parameter K, which was defined above, as the ratio between the dominant and the multipath component power. This parameter is given as follows:

$$K = \frac{A^2}{2\sigma^2}. \quad (6)$$

Using (6), it's possible rewrite (5) as a function of K only [11–13, 18]:

$$PDF(r) = \frac{r}{\sigma^2}\exp\left\{-\frac{r^2}{2\sigma^2}\right\}\exp(-K)I_0\left(\frac{r}{\sigma}\sqrt{2K}\right). \quad (7)$$

Using such presentation of Ricean PDF, one can easily obtain the mean value and the variance as functions of the parameter K, called also the *fading parameter*. Thus, according to definitions of the mean value and the variance [13, 14], is get:

$$\mu_r(K) = \int_0^\infty r \cdot PDF(r)\mathrm{d}r =$$
$$= \left[(1+K)I_0\left(\sqrt{2Kr}\right) + KI_1\left(K/2\right)\right]; \quad (8)$$

$$\sigma_r^2(K) = \int_0^\infty r^2 \cdot PDF(r)\mathrm{d}r = 2(1+K) - \mu_r^2. \quad (9)$$

Here, $I_1(\cdot)$ is the modified Bessel function of the first kind and first-order. For $K=0$: $\exp(-K)=1$ and $I_0(0)=1$, that is the worst case of the fading channel.

The Rayleigh PDF, when there is no LOS signal and is equal to:

$$PDF(r) = \frac{r}{\sigma^2}\exp\left\{-\frac{r^2}{2\sigma^2}\right\}. \quad (10)$$

Temporal and Spatial Error Concealment Methods

Temporal EC. In the natural form of a sequence of low resolution, the correlation between two consecutive frames is higher than the correlation of pixel values in the same block (frame) [22, 23]. Consequently, in most instances the temporal interpolation provides better means for masking errors than spatial interpolation.

If the remains are lost, but the motion vectors were taken correctly, the easiest way to decipher the missing blocks is to reset the missing remains to zero. This scenario occurs when data sharing is used. "Decoding without residues" method performs well if the missing remains are small. On the other hand, the residues are small if the sequence contains mainly linear movement, which can be easily predicted.

If all the information macroblock is lost, a simpler method, called the "copy-paste" method (also called zero-motion EC) [22], can be applied: the lost block is replaced by a spatially corresponding block in the previous frame. This method performs well only for sequences with low traffic. The best performance is provided by motor-compensated interpolation techniques. Methods for assessing the motion vector predicted the motion vector of the missing block in accordance with motion vectors of neighboring blocks (spatial — within one frame, or time — from previous frames).

Motion vector interpolation may lead to formation of blocking artifacts, especially in case of video sequences with non-uniform motion, and/or non-linear motion. Thus, in Chen et al. (1997) an improved method is provided. It sets weight in accordance with the "side match criterion". The side match criterion measures the difference between the pixel values at the boundary and inside the block, a motion vector obtained by interpolation. Parts with higher coincidence receive higher weights. In implementing substitutions, the side match criterion is used to select a motion vector — the vector of the block with the best side match is selected.

The motion vectors are correlated in the temporal domain in addition to the spatial one. Thus, besides the spatial interpolation of a motion vector, or in cases where spatially adjacent motion vectors are not available, temporary interpolation motion vector is the best one. The efficiency of a temporal interpolation of motion vector depends strongly on the temporal characteristics of the video stream. Performance of this interpolation method is greatly reduced as the frame rate decreases. Applying the average of the previous and subsequent frames may improve performance of the method, although it may lead to increased delay and storage.

Spatial EC. The spatial EC only uses information from the processed image to reconstruct the lost area. The quality of the reconstruction essentially depends on the spatial characteristics of the latent image, given only the distribution of edges [22, 23]. The approaches to concealment of missing parts with different spatial characteristics are not necessarily equal. While smooth portions may be interpolated by a simple averaging or by optimizing a cost function of smoothness, more complicated methods have to deal with regions containing edges [22, 23]. The smoothing should be done only along the edges, and the edges must be extended. The image resolution together with the size and shape of lost area determines solutions of an interpolation problem.

The simplest method of spatial EC is an interpolation of the missing block using the average value of the boundary pixel values. However, this leads to a monotonic interpolation of the block, indistinguishable from the rest of the picture, especially if the missing block is not smooth. The method of

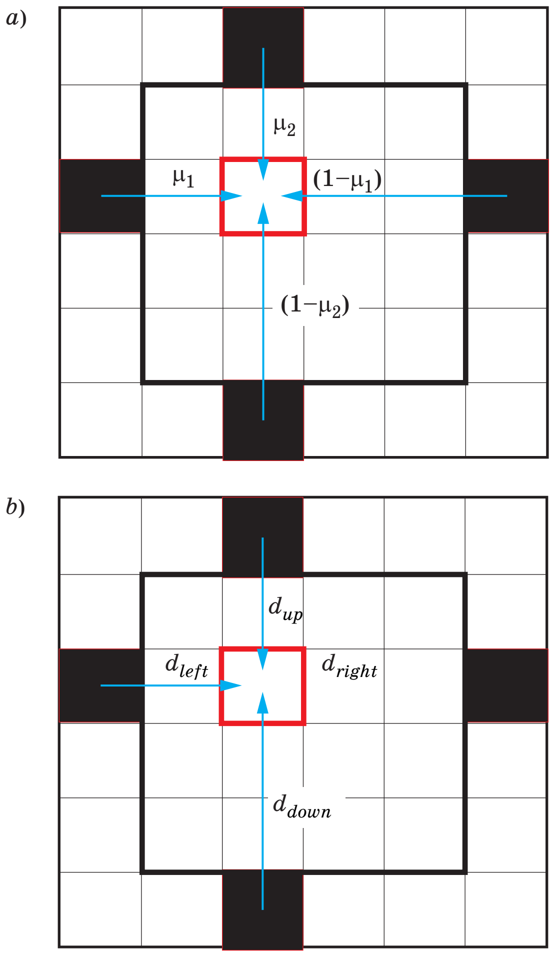

■ *Fig. 2.* Weighted Averaging: *a* — scheme 1; *b* — scheme 2

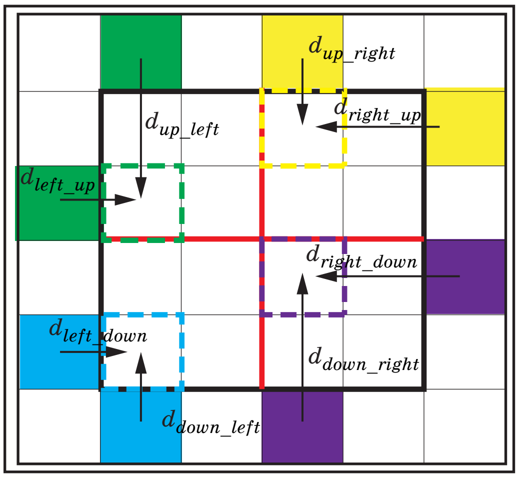

■ *Fig. 3.* Partial Weighted Averaging

“weighted average” (Sun and Reibmann, 2001) improves on average the previous weighting contributions boundary points, depending on the distance between the interpolated pixel and the other abroad (opposite boundary).

It should be noted that this method works well in restoring parts containing only one dominant direction. However, it does not provide satisfactory results, if a larger number of dominant edges are included in the lost region. Furthermore, if the intersecting edges of the missing block that are based on the aimed pixel are not linear, interpolation may lead to creation of unpleasant artifacts.

In our work we suggest the spatial method of EC. This method is compared to existing spatial techniques and to their variants which have been suggested during our research. These techniques are presented below.

Weighted Averaging. Weighted averaging is a method that recovers the missing pixel value by calculating the average pixel values from the four pixels in the four one-pixel wide boundaries of the damaged block weighted by the distance between the missing pixel and the four blocks boundaries (upper, down, left and right boundaries) as shown on Fig. 2, *a* and *b* [24]. The formula for calculating the missing pixel value (scheme 1) is:

$$P_{missed} = \frac{\left[\mu_1 \cdot P_{left} + (1-\mu_1) \cdot P_{right}\right]}{2} + \frac{\left[\mu_2 \cdot P_{up} + (1-\mu_2) \cdot P_{down}\right]}{2} \quad (11)$$

or (scheme 2):

$$P_{missed} = \left(d_{left} \cdot P_{left} + d_{right} \cdot P_{right} + d_{up} \cdot P_{up} + d_{down} \cdot P_{down}\right) / \left(d_{left} + d_{right} + d_{up} + d_{down}\right). \quad (12)$$

Partial Weighted Averaging. Partial Weighted Averaging method based on the original Weighted Averaging method. It recovers the missing pixel value by calculating the average pixel values from the two pixels in the two nearest one-pixel wide boundaries of the damaged block weighted by the distance between the missing pixel and the two blocks boundaries (upper and left, upper and right, down and right, down and left boundaries) as shown on Fig. 3. The formulas for calculating the missing pixels values are:

$$P_{missed\_left\_up} = \frac{d_{left\_up} \cdot P_{left\_up} + d_{up\_left} \cdot P_{up\_left}}{d_{left\_up} + d_{up\_left}};$$

$$P_{missed\_right\_up} = \frac{d_{right\_up} \cdot P_{right\_up} + d_{up\_right} \cdot P_{up\_right}}{d_{right\_up} + d_{up\_right}};$$

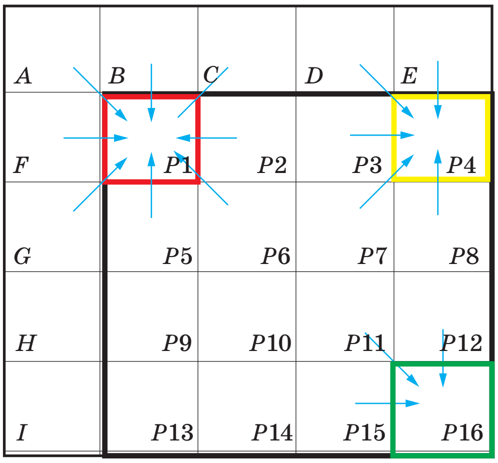

■ ***Fig. 4.*** Intra Prediction using System of Linear Equations by left top down scanning

$$P_{missed\_right\_down} = \left(d_{right\_down} \cdot P_{right\_down} + d_{down\_right} \cdot P_{down\_right}\right) / \left(d_{right\_down} + d_{down\_right}\right);$$

$$P_{missed\_left\_down} = \left(d_{left\_down} \cdot P_{left\_down} + d_{down\_left} \cdot P_{down\_left}\right) / \left(d_{left\_down} + d_{down\_left}\right). \quad (13)$$

Intra Prediction using System of Linear Equations (ISLE) *by left top down scanning*. Intra Prediction using System of Linear Equations uses the system of linear equations, which is a simple and effective tool applied almost everywhere [25, 26] for missing pixels value calculation. In the calculation, each pixel is the average of its nearest neighbours, when the top row and left column are known (pixels A–I on Fig. 4).

A $(N\times N)$-size block generates N^2 unknowns (number of pixels in lost block) and correspondingly N^2 equations, which are solved using the matrix representation. The formulas for calculating the missing pixels values for block on Fig. 4 are (clockwise from left top pixel):

$$P_1 = \frac{A+B+C+P_2+P_6+P_5+G+F}{8};$$

$$P_2 = \frac{B+C+D+P_3+P_7+P_6+P_5+P_1}{8};$$

$$P_3 = \frac{C+D+E+P_4+P_8+P_7+P_6+P_2}{8};$$

$$P_4 = \frac{D+E+P_8+P_7+P_3}{5};$$

$$P_5 = \frac{F+P_1+P_2+P_6+P_{10}+P_9+H+G}{8};$$

$$P_6 = \frac{P_1+P_2+P_3+P_7+P_{11}+P_{10}+P_9+P_5}{8};$$

$$P_7 = \frac{P_2+P_3+P_4+P_8+P_{12}+P_{11}+P_{10}+P_6}{8};$$

$$P_8 = \frac{P_3+P_4+P_{12}+P_{11}+P_7}{5};$$

$$P_9 = \frac{G+P_5+P_6+P_{10}+P_{14}+P_{13}+I+H}{8};$$

$$P_{10} = \frac{P_5+P_6+P_7+P_{11}+P_{15}+P_{14}+P_{13}+P_9}{8};$$

$$P_{11} = \frac{P_6+P_7+P_8+P_{12}+P_{16}+P_{15}+P_{14}+P_{10}}{8};$$

$$P_{12} = \frac{P_7+P_8+P_{16}+P_{15}+P_{14}}{5};$$

$$P_{13} = \frac{H+P_9+P_{10}+P_{14}+I}{8};$$

$$P_{14} = \frac{P_9+P_{10}+P_{11}+P_{15}+P_{13}}{5};$$

$$P_{15} = \frac{P_{10}+P_{11}+P_{12}+P_{16}+P_{14}}{5};$$

$$P_{16} = \frac{P_{11}+P_{12}+P_{15}}{3}. \quad (14)$$

Now there are 16 equations for 16 unknowns P_1–P_{16} which are solved using the matrix form of system of linear equations $A\mathbf{x}=B$, where vector $\mathbf{x}$ is P_1–P_{16}.

Intra Prediction using System of Linear Equations by symmetric scanning (ISLE). The Symmetric Intra Prediction using System of Linear Equations, as ISLE [25, 26], uses the system of linear equations for missing pixels value calculation. In the calculation, each pixel is the average of its nearest neighbours, when the top and bottom rows, and left and right columns are known (pixels A–T on Fig. 5).

Here, as in ISLE, $(N\times N)$-size block generates N^2 unknowns (number of pixels in lost block) and correspondingly N^2 equations, which are solved using the matrix representation. This technique is more effective than ISLE due to additional known information (additional known pixels). It should be noted that due to the symmetry, the number of the lost pixels changes.

The formulas for calculating the missing pixels values for block on Fig. 6 are (clockwise from left top pixel):

$$P_1 = \frac{A+B+C+P_2+P_4+P_3+S+T}{8};$$

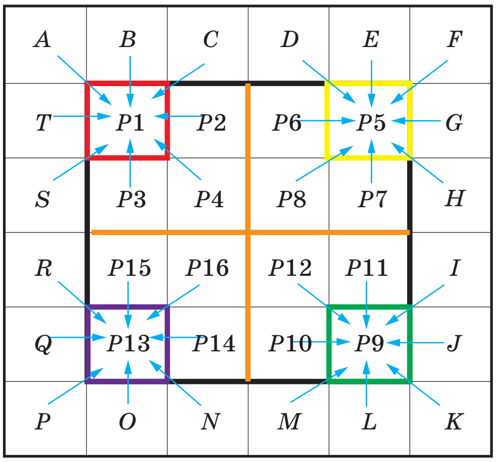

■ ***Fig. 5.*** Intra Prediction using System of Linear Equations by symmetric scanning

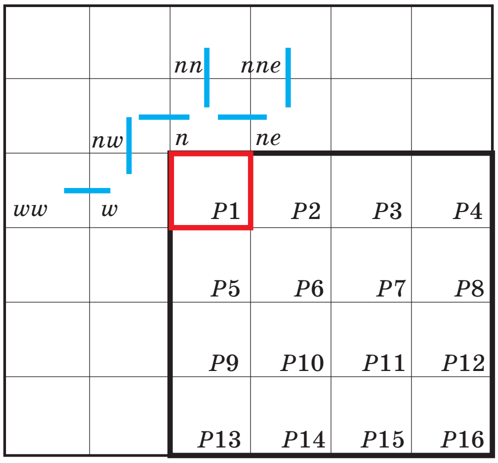

■ ***Fig. 6.*** Neighboring pixels used in prediction and modeling, and the estimated gradients of the image for standard CALIC by left top down scanning

$$P_2 = \frac{B + C + D + P_6 + P_8 + P_4 + P_3 + P_1}{8};$$

$$P_3 = \frac{T + P_1 + P_2 + P_4 + P_{16} + P_{15} + R + S}{8};$$

$$P_4 = \frac{P_1 + P_2 + P_6 + P_8 + P_{12} + P_{16} + P_{15} + P_3}{8};$$

$$P_5 = \frac{D + E + F + G + H + P_7 + P_8 + P_6}{8};$$

$$P_6 = \frac{C + D + E + P_5 + P_7 + P_8 + P_4 + P_2}{8};$$

$$P_7 = \frac{P_6 + P_5 + G + H + I + P_{11} + P_{12} + P_8}{8};$$

$$P_8 = \frac{P_2 + P_6 + P_5 + P_7 + P_{11} + P_{12} + P_{16} + P_4}{8};$$

$$P_9 = \frac{P_{12} + P_{11} + I + J + K + L + M + P_{10}}{8};$$

$$P_{10} = \frac{P_{16} + P_{12} + P_{11} + P_9 + L + M + N + P_{14}}{8};$$

$$P_{11} = \frac{P_8 + P_7 + H + I + J + P_9 + P_{10} + P_{12}}{8};$$

$$P_{12} = \frac{P_4 + P_8 + P_7 + P_{11} + P_9 + P_{10} + P_{14} + P_{16}}{8};$$

$$P_{13} = \frac{R + P_{15} + P_{16} + P_{14} + N + O + P + Q}{8};$$

$$P_{14} = \frac{P_{15} + P_{16} + P_{12} + P_{10} + M + N + O + P_{13}}{8};$$

$$P_{15} = \frac{S + P_3 + P_4 + P_{16} + P_{14} + P_{13} + Q + R}{8};$$

$$P_{16} = \frac{P_3 + P_4 + P_8 + P_{12} + P_{10} + P_{14} + P_{13} + P_{15}}{8}. \quad (15)$$

Now there are 16 equations for 16 unknowns P_1–P_{16} which are solved using the matrix form of system of linear equations $A\mathbf{x}=B$, where vector $\mathbf{x}$ is P_1–P_{16}.

Standard CALIC by left top down scanning. CALIC is the special framework that obtains higher lossless compression of continuous-tone images than other lossless image coding techniques mentioned in the literature [1]. This high coding efficiency is achieved with relatively low time and space complexities. CALIC is a sequential coding scheme that encodes and decodes in raster scan order with a single pass through the image. The coding process uses prediction and context templates that involve only the two previous scan lines of coded pixels. Consequently, the encoding and decoding algorithms require a simple two-line buffer that holds the two rows of pixels that immediately precede the current pixel.

Fig. 6 presents the neighboring pixels used in prediction and modeling, and the estimated gradients of the image, when P_1 is the first (in missed block) predicted pixel $I_p[i, j]$, let's mark it I_p. All the definitions and the prediction (that is concealment) showed in [1] and it is the procedure for left corner in our suggested modified method.

Mathematical and Statistical Description of Wireless Channel with Fading

Following [27, 28] we propose using the Ricean law, described by Ricean cumulative distribution function (CDF) and probability density function, for all the situations in the channel, including the worst and the best cases. From a practical point of view, the mean and the variance of Ricean distribution are used applying the Ricean fading parameter, K. Following expression (8), according to [29], for $K<2$:

$$\mu_r(K)=\sqrt{\frac{\pi}{2}}+\sum_{n=1}^{\infty}\frac{2}{\pi}\frac{(-1)^n}{(2n-1)!}K^n, \tag{16}$$

where as for $K\geq 2$:

$$\mu_r(K)=\sqrt{2K}\left(1-\frac{1}{4K}+\frac{1}{K^2}\right). \tag{17}$$

The same approximations can be obtained for the variance following derivations of expression (9) made in [29]. Thus, for $K<2$:

$$\sigma_r^2(K)=1-\left(\frac{\pi}{2}-1\right)\exp\left\{-\frac{K}{\sqrt{2}}\right\}, \tag{18}$$

where as for $K\geq 2$:

$$\sigma_r^2(K)=1-\frac{1}{4K}\left(1+\frac{1}{K}-\frac{1}{K^2}\right). \tag{19}$$

Using relations between the PDF and CDF, expression (10) allows us to obtain the Rayleigh CDF presentation:

$$CDF(R)\equiv \Pr(r\leq R)=\int_0^R PDF(r)\mathrm{d}r=$$
$$=1-\exp\left\{-\frac{R^2}{2\sigma_r^2}\right\}. \tag{20}$$

Using (7) for the Ricean PDF, there is a more difficult formula for Ricean CDF with respect to Rayleigh CDF due to summation of an infinite number of terms, such as:

$$CDF(R)=1-\exp\left\{-\left(K+\frac{r^2}{2\sigma_r^2}\right)\right\}\times$$
$$\times\sum_{m=0}^{\infty}\left(\frac{\sigma_r\sqrt{2K}}{r}\right)I_m\left(\frac{r\cdot\sqrt{2K}}{\sigma_r}\right). \tag{21}$$

Here $I_m(\cdot)$ is the modified Bessel function of the first kind and m-th order. Once more, the Ricean CDF depends only on parameter K and is limited to the Raleigh CDF and the Gaussian CDF for $K=0$ and for $K\to\infty$ respectively. Clearly, the CDF formula (21) is more complicated to evaluate analytically or numerically than the PDF formula (7). However, in practical terms, it is sufficient to use m up to the value where the last term's contribution becomes less than 0.1%. It was shown in [17] that for a Ricean CDF with $K=2$, the 14 dB of a fading outage probability is about 10^{-2}.

New method for the determining of BER in Ricean fading channel is offered by [30]. In order to calculate the BER, this method uses level crossing rate (LCR) and average fade duration (AFD).

Level crossing rate, N_x, is the expected rate at which the received signal envelope crosses the threshold in a positive-going or negative-going direction [31]. AFD, $<\tau>$, is the average period of time for which the receiver signal envelope is below a threshold X [31]. We present the formulas of the LCR and the AFD according to [32]. The LCR formula is:

$$N_x(X)=\frac{2X\sqrt{2\varsigma}}{\pi^{3/2}K(0)}e^{-\left(X^2+\rho^2\right)/K(0)}\times$$
$$\times\int_0^{\pi/2}\cosh\left(\frac{2X\rho\cos\alpha}{K(0)}\right)\times$$
$$\times\left[e^{-\xi\rho\sin\alpha}+\sqrt{\pi}\xi\rho\sin\alpha Q(\xi\rho\sin\alpha)\right]\mathrm{d}\alpha, \tag{22}$$

where X is the level of the received input signal (threshold); $Q(\cdot)$ is the error function [29, 31, 33]:

$$Q(w)=\frac{1}{2}\mathrm{erf}\left\{\frac{w}{\sqrt{2}}\right\}, \tag{23}$$

where

$$\mathrm{erf}\{w\}=\frac{2}{\sqrt{\pi}}\int_0^w e^{-y^2}\mathrm{d}y; \tag{24}$$

ρ is the amplitude of the LOS component of the signal strength [31]:

$$\rho=\sqrt{\frac{K}{K+1}}; \tag{25}$$

σ is the standard deviation [31]:

$$\varsigma=-\frac{1}{2}K''(0)-\frac{\mathrm{Im}\{K'(0)\}^2}{2K(0)} \tag{26}$$

and ξ is presented from [31] by the following expression:

$$\xi=\frac{\left[\omega_D\cos\alpha_0-\frac{\mathrm{Im}\left\{K'(0)\right\}}{K(0)}\right]}{\sqrt{2\varsigma}}, \tag{27}$$

where α and α_0 are the angle and the initial angle between the transmitting and receiving antennas and the functions $K(0)$, $K'(0)$ and $K''(0)$ are defined in [32] as:

$$K(0)=\frac{1}{K+1};$$

$$K'(0) = -\frac{i\omega_D}{K+1}\left[\frac{\cos\theta \cdot I_1(k)}{I_0(k)}\right];$$

$$K''(0) = \frac{\omega_D^2}{2(K+1)}\left[1 + \frac{\cos 2\theta \cdot I_2(k)}{I_0(k)}\right], \quad (28)$$

where K (K-factor) is one of inputs that defines the relative strength of LOS component and the multipath scattered component; $I_n(k)$, $n=1, 2, 3, ...$ are the n-th order modified Bessel functions of the first kind; k is the beamwidth of arriving waves, θ is the angle between the average scattering direction and the mobile vehicle direction.

The AFD can be defined as:

$$<\tau> = \frac{1}{N_x} CDF(X), \quad (29)$$

where $CDF(X)$ is the probability of the event in which the received signal envelope does not exceed a specific level X, that is:

$$CDF(X) = \frac{1}{T}\sum_{i=1}^{n} \tau_i, \quad (30)$$

where τ_i is the duration of the fade and T is the observation interval of the fading signal (see Fig. 7), when:

$$N_x = \sum_m^M n_{x_m}. \quad (31)$$

After inserting the (30) in the (28), the resulting AFD defines percent of the bit time duration affected by Ricean fading. In order to calculate the BER the following formula is used:

$$BER \equiv P_6 = \frac{number\ of\ bits\ in\ error\ per\ second}{number\ of\ bits\ in\ data\ per\ second} \quad (32)$$

in which the number of bits in data per second constitutes the rate (R) of bit stream and the number of bits in error per second constitutes the LCR [31]. Put differently, LCR is the number of crosses per second, N_x. Therefore, (32) can be written as:

$$BER = \frac{N_x}{R}. \quad (33)$$

In further computations the above formula is used to estimate the BER in the channel with the Ricean fading. It is necessary to note that the LCR (N_x) is a general expression for the envelope LCR and contains the formula of Rayleigh N_x from [29, 34, 35], taking into account as well the notion that it is a formula of LCR for the channel with Rayleigh fading:

$$N_x = \sqrt{2\pi} f_m \varsigma e^{-\varsigma^2}. \quad (34)$$

Thus, (22) contains a special case of Rayleigh fading, usually used for Doppler effect estimation through the LCR estimates [19, 36, 37]. On this basis, it can be assumed that the formula of BER calculating for the channel with Ricean fading using different K-factor values allows us to get the BER of the channel with Rayleigh fading (low K) and the BER of the channel with Gaussian fading (high K). It follows that Ricean distribution law covers both the Rayleigh and Gauss laws. This is achieved by using the Ricean parameter of fading, K, which in situations of bad clearance between two terminals ($K \to 0$) transforms Ricean CDF and PDF to their Rayleigh counterparts [described by (10)], and in situations of good clearance between two terminals without any multipath components ($K \to \infty$) transforms Ricean CDF and PDF to their Gaussian counterparts yielding "Dirac-delta shaped" PDF [described by (1)] (Fig. 8) [29].

Such it is clear that the Ricean channel behaves like AWGN channel in the limit as $K \to \infty$, and like Rayleigh multipath channel when $K=0$ or $K \to 0$.

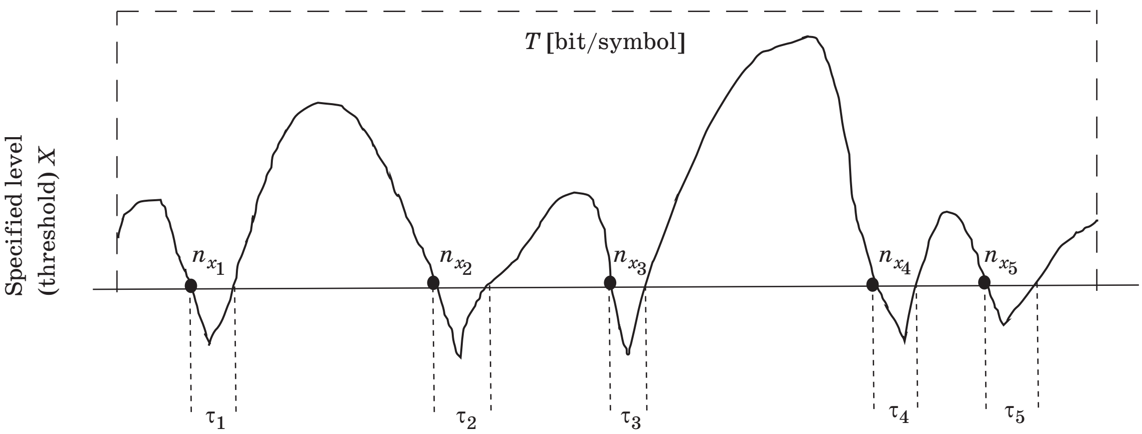

■ ***Fig. 7.*** The illustration of definitions of the signal fading statistical parameters LCR and AFD

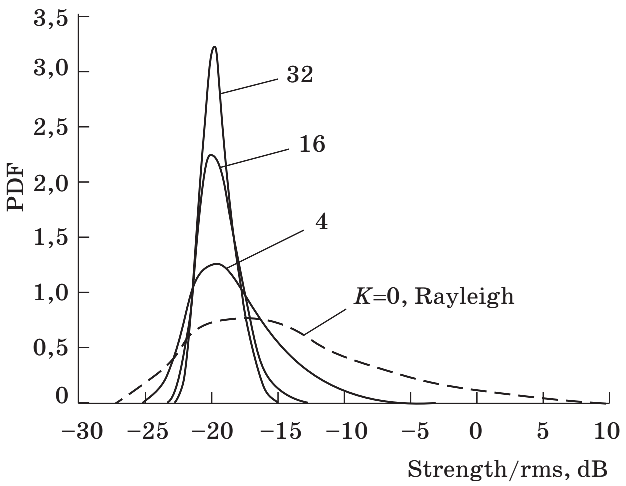

■ *Fig. 8.* Ricean PDF distribution versus ratio of signal to rms

It should be noted that the using of the formula for calculating the BER in the Ricean channel with the aim of receiving BER of AWGN and Rayleigh channels is logical and convenient, because usually there exists a spectrum of “average” cases with “medium” levels of noise, interferences and errors. These average cases produce the Ricean channel, and in “extreme” cases it is possible to quickly get the BER for Rayleigh and Gaussian channels without changing the concept.

To demonstrate the veracity of the BER, calculated using LCR formula for three models of channels, the graph has been constructed. This graph demonstrates that different values of K are obtained curve BER. The graph also shows that a low K leads to the BER closer to Rayleigh case, while a high K leads to the BER closer to Gauss occasion. All the results are shown and described in the Part 2.

References

1. Wu X., and Memon N. CALIC — a Context Based Adaptive Lossless Image Codec. *Proc. Int. Conf. on Acoust., Speech, Signal Processing*, Atlanta, GA, May 1996, pp. 1891–1894.
2. Zhao X., Lu H., Chen C. W., and Wu J. Adaptive Hybrid Digital-analog Video Transmission in Wireless Fading Channel. *IEEE Trans. on Circuits and Systems for Video Technology*, 2016, no. 6, pp. 1215–1223.
3. Shen X., Tang L., and Zhang X. A Video Transmission Scheme Based on Scalable Video Coding over MIMO Wireless Systems. *Intern. Conf. on Wireless Communication and Sensor Network*, 2014, 6 p.
4. Purandare R. G., Kshirsagar S. P., Kol S. M., and Gohokar V. V. Impact of Bit Error on Video Transmission over Wireless Networks and Error Resiliency. *Intern. Conf. on Image Information Processing* (*ICIIP*), 2011, 6 p.
5. Bocus M. Z., and Coon J. P. *Rate-Optimization for Scalable Video Transmission over Wireless Networks*. IEEE Press, 2014. 287 p.
6. Hadar O., Huber M., and Huber R. Hybrid Error Concealment with Automatic Error Detection for Transmitted MPEG-2 Video Streams over Wireless Communication Network. *Intern. Conf. on Information Technology: Research and Education*, 2006, 6 p.
7. Hadar O., Huber M., Huber R., and Greenberg S. New Hybrid Error Concealment for Digital Compressed Video. *EURASIP Journal on Applied Signal Processing*, 2005, no. 6, pp. 1821–1833.
8. Mazataud C. *Error Concealment for H.264 Video Transmission*. A Thesis Presented to the Academic Faculty, In Partial Fulfillment of the Requirements for the Degree of Master of Science in the School of Electrical and Computer Engineering, Georgia Institute of Technology, 2009. 94 p.
9. Patel D., and Patel J. Hybrid Spatio-Temporal Error Concealment Technique for Image/Video Transmission. *IEEE Proc.*, 2014, no. 5, pp. 814–823.
10. Lee Y. H., and Wu T. H. Video Error Concealment Using Progressive Block Matching Algorithm with Euclidean Distance. *Eighth Intern. Conf. on Intelligent Information Hiding and Multimedia Signal Processing*, 2012, 6 p.
11. Jakes W. C. *Microwave Mobile Communications*. New York, John Wiley & Son, 1974. 480 p.
12. Steele R. *Mobile Radio Communication*. IEEE Press, 1992. 395 p.
13. Stuber G. L. *Principles of Mobile Communications*. Boston-London, Kluwer Academic Publishers, 1996. 497 p.
14. Blaunstein N., and Andersen J. B. *Multipath Phenomena in Cellular Networks*. Boston-London, Artech Houses, 2002. 296 p.
15. Saunders S. R. *Antennas and Propagation for Wireless Communication Systems*. New York, John Wiley & Sons, 1999. 409 p.
16. Bertoni H. L. *Radio Propagation for Modern Wireless Systems*. New Jersey, Prentice Hall PTR, 2000. 258 p.
17. Blaunstein N. *Wireless Communication Systems*. Chapter 12. In: *Handbook of Engineering Electromagnetics*. Ed. by Rajeev Bansal. New York, Marcel Dekker, 2004. 67 p.
18. Rappaport T. S. *Wireless Communications*. New York, Prentice Hall PTR, 1996. 642 p.
19. Lee W. Y. C. *Mobile Cellular Telecommunications Systems*. New York, McGraw Hill, 1989. 563 p.
20. Leon-Garcia A. *Probability and Random Processes for Electrical Engineering*. New York, Addison-Wesley Publishing Company, 1994. 349 p.
21. Stark H., and Woods J. W. *Probability, Random Processes, and Estimation Theory for Engineers*. New Jersey, Prentice Hall, 1994. 376 p.

22. Goldsmith A. J., and Chua S. G. Variable-Rate Variable-Power MQAM for Fading Channels. *IEEE Trans. Communic.*, 1997, no. 11, pp. 1218–1230.
23. Chen T. P.-C., and Chen T. Second-Generation Error Concealment for Video Transport over Error-Prone Channels. *Wireless Communic. and Mobile Computing*, 2002, no. 4, pp. 607–624. doi:10.1002/wcm.83
24. Sun M. T., and Reibman A. R. *Compressed Video over Networks*. New York, Marcel Dekker, 2001. 358 p.
25. Doshkov D., Ndjiki-Nya P., Lakshman H., Koppel M., and Wiegand T. Towars Efficient Intra Prediction Based on Image Impainting Methods. *28th Picture Coding Symp., PCS2010*, December 8–10, 2010, Nagoya, Japan, 6 p.
26. Chen B. N., and Lin Y. Selective Motion Field Interpolation for Temporal Error Concealment. *Intern. Conf. on Computer and Communication Engineering 2006 (ICCCE 2006)*, Kuala Lumpur, Malaysia, May 9–11, 2006, 6 p.
27. Blaunstein N., Arnon S., Zilberman A., and Kopeika N. *Applied Aspects of Optical Communication and LIDAR*. Taylor and Francis Group, 2010. 262 p.
28. Blaunstein N. *Radio Propagation in Cellular Networks*. Boston-London, Artech House, 2000. 386 p.
29. Blaunstein N., and Christodoulou C. G. *Radio Propagation and Adaptive Antennas for Wireless Communication Networks*. New Jersey, John Wiley & Sons, 2007. 614 p.
30. Blaunstein N., and Yarkoni N. Data Stream Parameters Prediction in Land and Atmospheric MIMO Wireless Communication Links with Fading. *2nd European Conf. on Antennas and Propagation (EUCAP 2007)*, Edinburgh, November 2007, pp. 123–126.
31. Tepedelenlioglu C., et al. Estimation of Doppler Spread and Spatial Strength in Mobile Communications with Applications to Handoff and Adaptive Transmissions. *J. Wireless Communic. Mobile Computing*, 2001, no. 2, pp. 221–241.
32. Goldsmith A. J. *Wireless Communications*. New Jersey, Wiley & Sons, 2004. 419 p.
33. *Modulation and Coding Techniques in Wireless Communications*. Ed. by E. Krouk and S. Semenov. United Kingdom, Wiley, 2011. 662 p.
34. Katz B., Greenberg S., Yarkoni N., Blaunstien N., and Giladi R. New Error-Resilient Scheme Based on FMO and Dynamic Redundant Slices Allocation for Wireless Video Transmission. *IEEE Trans. on Broadcasting*, 2007, no. 1, pp. 127–135.
35. Rappaport T. S. *Wireless Communications Principles and Practice*. New York, Prentice Hall, 1996. 452 p.
36. Blaunstein N., and Cristodoulou Ch. *Radio Propagation and Adaptive Antennas for Wireless Communication Networks*. New Jersey, Hoboken, John Wiley & Sons, 2014. 683 p.
37. Molisch A. F. *Wireless Communications*. London, Wiley and Sons, 2006. 622 p.

УДК 621.39
doi:10.15217/issn1684-8853.2017.1.72

Оптимизация маскирования ошибок на основе анализа затухания типов фадинга
Часть 1: Статистическое описание беспроводного видеоканала, модели определения BER и маскирования ошибок видеосигналов

Хадар Офер[а], Phd, доцент
Бронфман Ирина[б], MSc студент
Блаунштейн Натан[а,б], доктор физ.-мат. наук, профессор
[а]*Негевский университет им. Бен-Гуриона, г. Беэр-Шева, Израиль*
[б]*Иерусалимский технологический институт, Иерусалим, Израиль*

Цель исследования: представить наиболее эффективный метод расчетов параметров канала с затуханием и разработать методы достижения лучшего и более эффективного выполнения замещения ошибок, что повысит качество видео после прохождения через канал с затуханием. **Методы:** исследованы влияние затухания на канал связи при помощи изучения распределений Гаусса, Рейли и Райса, а также существующие методы прогнозирования и замещения ошибок и их влияние на качество видео после выхода из канала с затуханием. **Результаты:** показано, что распределение Райса более широкое и охватывает другие виды распределения — Гаусса (идеальный канал) и Рейли (канал с затуханием), поэтому, именно это распределение было использовано для тестирования практических случаев, возникающих в видеоканале. По теме замещения ошибок проведена оптимизация метода CALIC, названная Симметричный CALIC (Symmetric CALIC). Реализовано сравнение данной оптимизации с оригинальным методом CALIC и с другими методами и определено, что предлагаемая оптимизация показывает лучшие результаты, чем все использованные для сравнения методы. Предложен новый метод замещения ошибок, названный Сбалансированным Процентарным Расчетом (Balanced Percentage Calculation), в сравнении показавший в среднем в два раза лучшие результаты, чем Симметричный CALIC, и намного лучшие результаты, чем остальные использованные для сравнения методы. Две темы объединены таким образом, что затухание повлияло на появление в видеофайле ошибок, которые были исправлены при помощи предложенных методов замещения ошибок. Все практические тесты и сравнения проведены в MatLab. **Практическая значимость:** предложенный способ расчета параметров канала с затуханием позволяет выполнять расчеты для любых видов каналов, что значительно облегчает работу с каналами в общем и с необходимыми для них расчетами в частности. Предложенные оптимизация существующего метода замещения ошибок и новый метод замещения ошибок позволяют получать видео более высокого качества после прохождения через канал с затуханием.

Ключевые слова — распределение Райса, затухание Райса, скорость ошибочных битов, BER, замещение ошибок, коэффициент уровня пересечения, средняя продолжительность затухания, CALIC, симметричный CALIC, сбалансированный процентарный расчет, средняя взвешенность, внутрикадровое прогнозирование с помощью системы линейных уравнений.